Theoretical Studies of the Kinetic and Thermodynamic Stabilities of Isomers of HXGeS (X = H, F, Cl, and Br) in the Gas Phase

Chiu-Ling Lin,[†] Ming-Der Su,*,[‡] and San-Yan Chu*,[†]

Department of Chemistry, National Tsing Hua University, Hsinchu 30043, Taiwan, ROC, and School of Chemistry, Kaohsiung Medical University, Kaohsiung 80708, Taiwan, ROC

Received: May 18, 2000; In Final Form: July 20, 2000

Potential energy surfaces for the unimolecular decomposition reactions of HXGe═S (X = H, F, Cl, and Br) have been explored using B3LYP and CCSD(T) calculations. Five different reaction mechanisms are proposed: (A) 1,1-HX elimination, (B) 1,2-H shift, (C) 1,2-X shift, (D) H and XGeS radical formation, and (E) X and HGeS radical formation. According to our theoretical investigations, as in the case of HXGe═O, HXGe═S is found to be kinetically stable with respect to the unimolecular destruction reactions, despite its thermodynamic instability. Furthermore, the stabilization energies, which indicate the extent to which halogen substitution stabilizes the Ge═S double bond, increase along the series X = F, Cl, Br, and H and show a reasonable linear correlation with the electronegativity of the halogen.

I. Introduction

The possible existence of π-bonded germane intermediates has been attracting a great deal of attention in organogermane chemistry over the last two decades.[1,2] Germanium−germanium, germanium−carbon, germanium−silicon, and germanium−oxygen double bonds in particular have been well-studied both experimentally and theoretically.[3−6] It is natural that current interest is directed toward the preparation of germanium−sulfur doubly bonded compounds, germanethiones (RR′Ge═S).[7,8] In fact, recent years have witnessed several reports on the generation and reaction of germanethiones.[9−11] It is generally agreed that germanethiones are notoriously unstable unless encumbered by sterically demanding substituents.[1,2] It is not surprising that the first kinetically stabilized germanethione to be isolated and crystallographically analyzed was made only seven years ago.[12] Its stabilization in a monomeric state was achieved by the use of bulky substituents on the germanium atom.

As such, the reactive nature of the germanethione species makes it difficult to obtain quantitative physical parameters, e.g., energies and geometries, experimentally. Such molecules are therefore amenable to accurate theoretical investigations, and it is desirable to explore the possibility and opportunity to obtain reliable information in this manner. To gain some insight into the stability of germanethione and its derivatives, we have undertaken a theoretical investigation of the unimolecular decomposition reactions of HXGe═S (X = H, F, Cl, and Br). To our knowledge, only the parent H_2Ge═S species has been the subject of previous theoretical treatments.[13−16] Of these, the most recent and comprehensive study has been that by Nowek, Sims, Babinec, and Leszczynski.[16] These authors used the QCISD(T)/TZP++(2df,2pd) level of theory to investigate three of the singlet isomers considered here, H_2Ge═S, *trans*-HGeSH, and *cis*-HGeSH. Likewise, no theoretical study concerning the structural and energetic effects of monohalogen-substituted germanethiones has appeared to date. It is believed that in view of recent dramatic developments in gemanethione chemistry,[1,2] analogous extensive studies of molecules with a Ge═S double bond should soon be forthcoming and will open up new areas.

SCHEME 1

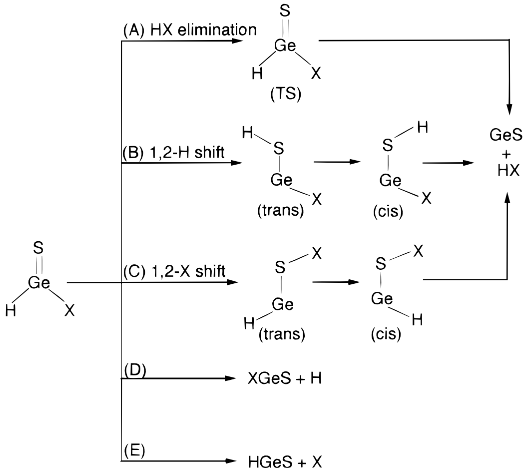

The unimolecular reactions pertinent to the stability of HXGe═S are shown in Scheme 1. Namely, the reactions considered here are (A) the single-step elimination of HX, (B) the 1,2-hydrogen shift, (C) the 1,2-halogen shift, (D) the formation of XGeS and H radicals, and (E) the formation of HGeS and X radicals. In other words, the purpose of the present work is to provide the theoretical information about the relative stabilities of HXGe═S (X = H, F, Cl, and Br) and its isomers. Moreover, we also report theoretical predictions of the molecular parameters and vibrational frequencies of HXGe═S species, which should be useful for further experimental observations.

II. Computational Methods

All calculations were carried out using the Gaussian 98 series of programs.[17] The geometries of all of the species were fully optimized using the hybrid density functional method B3LYP/6-311G* (hereafter designed B3LYP).[18] Vibrational frequency

---

[†] National Tsing Hua University.

[‡] Kaohsiung Medical University.

10.1021/jp0018302 CCC: $19.00

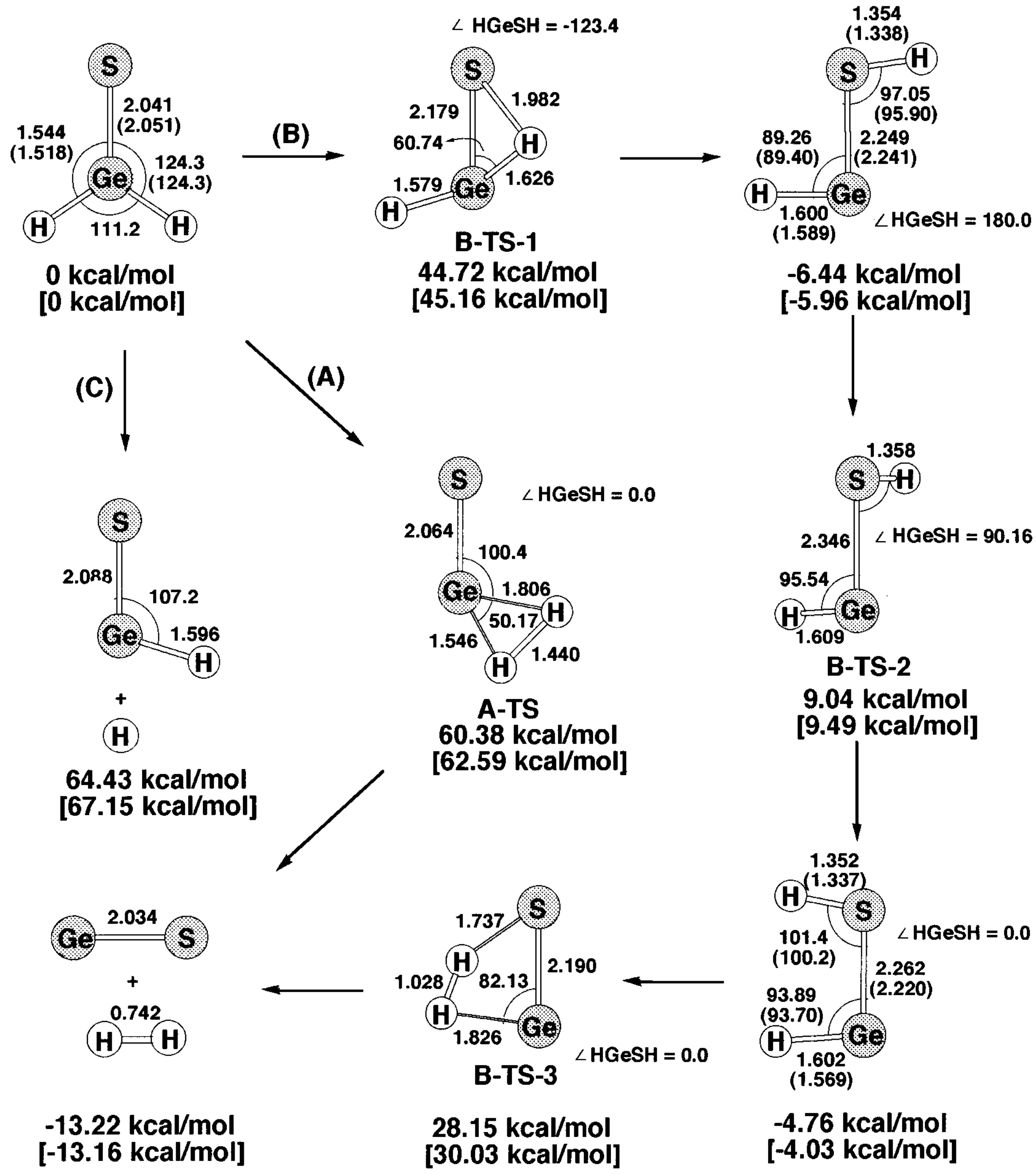

Figure 1. B3LYP/6-311G* optimized geometries (in Å and deg) and relative energies for the $H_2Ge{=}S$ isomers. Values in parentheses are taken from the previous calculations (ref 16). Values in brackets are at the CCSD(T) level of theory (see the text).

calculations at the B3LYP/6-311G* level were used to characterize all stationary points as either minima (the number of imaginary (NIMAG) = 0) or transition states (NIMAG = 1). Additionally, the vibrational zero-point energy (ZPE) corrections determined at the B3LYP/6-311G* level are also included, i.e., B3LYP/6-311G* + ZPE (B3LYP/6-311G*). For better energetics, single-point energies were also calculated at CCSD(T)/6-311++G(d,p)//B3LYP/6-311G* + ZPE (B3LYP/6-311G*) (hereafter designed CCSD(T)),[19] to improve the treatment of electron correlation.

III. Results and Discussion

(1) $H_2Ge{=}S$ Decomposition Reactions. In the case of $H_2Ge{=}S$, there are three kinds of dissociation pathways, i.e., (A) 1,1-hydrogen elimination, (B) 1,2-hydrogen shift, and (C) radical dissociation. The optimized geometries, calculated at the B3LYP/6-311G* level of theory, for the intermediates and transition states of the above reaction channels are shown in Figure 1. The predicted geometrical parameters (bond lengths and bond angles) for $H_2Ge{=}S$ as well as the calculated vibrational frequencies, dipole moments, atomic charges, and rotational constants are given in Table 1, where they are compared with previous theoretical calculations.[13−16] Also, the calculated molecular parameters of $H_2Ge{=}S$ and its isomers at B3LYP and CCSD(T) levels of theory are collected in Table 2.

At present, no experimental data for $H_2Ge{=}S$ and its isomers are available for comparison. Due to this, the reliability of the predicted geometries can be assessed only by comparison between different levels of theory. As mentioned earlier, the most recent theoretical values (QCISD(T)/TZP++(2df,2pd)) for $H_2Ge{=}S$, *trans*-HGeSH, and *cis*-HGeSH species were obtained by Leszczynski, Nowek, Sims, and Babinec.[16] As one can see in Figure 1 and Table 1, the molecular parameters of $H_2Ge{=}S$ for our B3LYP calculations compare well with the QCISD(T) results. The bond lengths and angles are in agreement to within 0.02 Å and 0.5°, respectively. Furthermore, our energies based on the CCSD(T) calculations are in good agreement with theirs. The relative energies for $H_2Ge{=}S$, *trans*-HGeSH, and *cis*-

TABLE 1: Molecular Parameters of Germanethione Based on This Work Compared with the Previous Calculations

	this work[a]	calc[b]
r(Ge−S) (Å)	2.041	2.051
r(Ge−H) (Å)	1.544	1.518
∠ HGeS (deg)	124.3	124.3
vibrational mode (cm^{-1})[c]		
ν_1(C−H asym str), B_1	2073	
ν_2(C−H sym str), A_1	2082	
ν_3(H−Ge−H bend), A_1	523	
ν_4(H_2GeS wag), B_2	521	
ν_5(H_2GeS rock), B_1	880	
ν_6(Ge=S str), A_1	553	
dipole moment (Debye)	3.18	
rotational constants (MHz)		
A	154375.21	
B	5189.10	
C	5020.35	
atomic charges		
q(Ge)	0.2786	
q(S)	−0.3099	
q(H)	0.01569	

[a] B3LYP/6-311G*; see the text. [b] QCISD(T)/TZP++(2df,2pd); see ref 16. [c] Without scaling.

HGeSH are (0.0, −6.0, −4.0) kcal/mol from our results in comparison with their values of (0.0, −5.2, −3.5) kcal/mol. It has to be emphasized that our calculated Ge=S double bond length (2.041 Å for H_2GeS) is in good agreement with the experimental one (2.049 Å for Tbt(Tip)Ge=S).[12b] As a result of this good agreement on the known singlet-state features, we are confident that the computational methods used in this study are reliable.

For reaction path (A), **H_2GeS-A-TS** is the transition state for 1,1-hydrogen elimination leading to H_2 + GeS. The B3LYP results indicate that this transition structure is planar with both hydrogen atoms on the same side of the GeS bond axis. The CCSD(T) results predict that this reaction path (A) is exothermic (−13 kcal/mol) and possesses a sizable energy barrier (63 kcal/mol).

For reaction path (B), **H_2GeS-B-TS-1** and **H_2GeS-B-TS-2** are the transition structures for the 1,2-hydrogen shift in H_2Ge=S to HGeSH and the trans to cis isomerization of HGeSH. Both are calculated to be nonplanar. **H_2GeS-B-TS-3** is the transition structure for the molecular dissociation of *cis*-HGeSH leading to H_2 + GeS, which is planar. As seen in Figure 1, H_2Ge=S is 6.0 and 4.0 kcal/mol less stable than *trans*-HGeSH and *cis*-HGeSH, respectively. Additionally, the inter-rotation of HGeSH leads to the formation of the two planar trans and cis isomers, i.e., *trans*-HGeSH and *cis*-HGeSH. Both of these forms were found to be minima on the B3LYP and CCSD(T) potential energy surfaces. The main difference between the computed geometries concerns the bond angles HSGe and HGeS, respectively. They are consistently larger for the cis isomer by 4° and 5°, respectively. Differences were also found in the bond distances. With regard to the energetics, the trans isomer is estimated to be ca. 1.9 kcal/mol (CCSD(T)) more stable than the cis one. It should be stressed that there exists a high activation barrier (45 kcal/mol at CCSD(T)) between H_2Ge=S and the HGeSH isomers. As a consequence, if H_2Ge=S and/or HGeSH isomers were formed directly by the appropriate gas-phase experiments, they should not easily interconvert. In addition, the internal rotational transition state (**H_2GeS-B-TS-2**) lies 14 kcal/mol above *trans*- and *cis*-HGeSH, and also 9.5 kcal/mol above H_2Ge=S. Thus, the thermal intramolecular rearrangement (*trans*-HGeSH → *cis*-HGeSH) is expected to be a facile process. Moreover, the barrier height for the dissociation *cis*-HGeSH → H_2 + GeS is 30 kcal/mol above germanethione, but still lower than the barrier height (45 kcal/mol) for the reaction H_2Ge=S → *trans*-HGeSH. This suggest that when the 1,2-hydrogen shift occurs, it is likely to be followed by the generation of H_2 and GeS via the transiency of HGeSH. It is worth noting that the energy difference between H_2Ge=S and *trans*-HGeSH is as small as 6.0 kcal/mol, which is in distinct contrast to the much larger energy difference (21 kcal/mol) favoring *trans*-HGeOH over H_2Ge=O.[6] In any event, the relative stability of the double-bonded and the divalent species is a general feature of germane compounds and indicates that germane is reluctant to form doubly bonded compounds. Furthermore, as noted above, the decomposition of H_2Ge=S to HGeSH and subsequently to H_2 + GeS still requires substantial activation energy (at least > 30 kcal/mol at CCSD(T)). This finding strongly imply that H_2Ge=S is stable in a kinetic sense despite its thermodynamic instability (vide infra).

In addition to reaction paths (A) and (B), there exists a third channel (C), i.e., the elimination of a hydrogen atom from H_2Ge=S giving the HGeS radical. Our calculations predict that the reaction (C) is strongly endothermic (67 kcal/mol at CCSD(T)), implying that this reaction pathway is energetically unfavorable. In consequence, in the competition of the 1,1-hydrogen elimination (A) with the 1,2-hydrogen shift (B) and the dissociation process (C), reaction (B) has the lowest energy requirement and thus is the most energetically favorable pathway of the H_2Ge=S unimolecular decomposition reactions.

(2) HFGe=S Decomposition Reactions. In the case of HFGe=S, there are five kinds of reaction routes as given in Scheme 1. Namely, (A) 1,1-HF elimination, (B) 1,2-hydrogen shift, (C) 1,2-fluorine shift, (D) formation of FGeS and H radicals, and (E) formation of HGeS and F radicals. The fully optimized geometries of the equilibrium structures and transition states are presented in Figure 2. The calculated vibrational frequencies as well as dipole moment, rotational constants, atomic charges and relative energies of HFGe=S and its derivatives are collected in Table 3. While there are no experimental values available for HFGe=S structural parameters to compare with the calculated values, we believe that the structures of the HFGe=S species are also well described at the B3LYP/6-311G* level of theory.

Our computational results for the HFGe=S reactions are in many respects similar to those discussed earlier for the H_2Ge=S system. However, several intriguing results may be drawn from Figure 2 as follows.

First, as seen in Figure 2, the CCSD(T) results predict that energy of *trans*-FGeSH is apparently lower than that of HFGe=S by 16 kcal/mol, while *cis*-FGeSH is 0.04 kcal/mol lower than *trans*-FGeSH. This small energy separation between the FGeSH isomers makes the assignment of the FGeSH singlet state structure uncertain. Moreover, the internal rotational transition state (i.e., **FGeSH-B-TS-2**) lies 7.0 kcal/mol below HFGe=S. Accordingly, this finding suggests that the intramolecular rearrangement (*trans*-FGeSH → *cis*-FGeSH) should proceed without activation.

On the other hand, trans and *cis*-HGeSF (1,2-F shifted isomers) possess the highest energy of all the minima on the HFGe=S surface at both computational levels employed. The average energy difference between HGeSF and HFGe=S is 41 (B3LYP) and 44 (CCSD(T)) kcal/mol. Moreover, the CCSD(T) calculations predict that the activation barrier for the 1,2-F migration (C) is sizable (at least >55 kcal/mol). Such a substantial barrier for the isomerization of HGeSF can be easily understood in terms of repulsion between the F electron lone

TABLE 2: Calculated Vibrational Frequencies (cm^{-1}), IR Intensity (KM/mol), Rotational Constants (MHz), Dipole Moments (Debye), Atomic Charges, and Relative Energies (kcal/mol) of the Species in H_2GeS Decomposition Reactions at the B3LYP/6-311G* Level of Theory

species	frequency[a] (IR intensity)	rotational constants	dipole moment	*q*(Ge)	*q*(S)	*q*(H)	relative energies
$H_2Ge{=}S$	2082(138),2073(72), 880(100), 553(26), 523(16), 521(7)	A 154375.21 B 5189.10 C 5020.35	3.180	0.2786	−0.3099	0.01569	0.0 (0.0)[b]
H_2GeS-A-TS	2086, 1335, 529, 470, 426, 1503i						60.38 (62.59)
H_2GeS−B-TS-1	1921, 1730, 682, 478, 412, 1266i						44.72 (45.16)
trans-HGeSH	2608(8), 1882(307), 856(18), 599(11), 571(2), 379(40)	A 117626.02 B 4338.30 C 4183.98	1.405	0.1799	−0.2646	−0.06192(Ge) 0.1466(S)	−6.44 (−5.96)
H_2GeS−B-TS-2	2581, 1825, 699, 534, 328, 699i						9.04 (9.49)
cis-HGeSH	2617(4), 1861(329), 757(34), 629(10), 499(28), 371(46)	A 118744.86 B 4270.54 C 4122.29	1.231	0.2015	−0.2880	−0.07471(Ge) −0.1612(S)	−4.76 (−4.03)
H_2GeS−B-TS-3	1568, 1509, 975, 878, 451, 1575i						28.15 (30.03)
GeS + H_2	GeS: 566(47) H_2: 4395(0)	GeS: 5469.38 H_2:1822596.708	GeS: 2.513				−13.22 (−13.16)
HGeS	1817(111), 525(23), 362(9)	A 220691.57 B 5127.94 C 5011.49		0.2188	−0.2410	0.005315	

[a] Without scaling. [b] Values in parentheses are based on the CCSD(T) level of theory; see the text.

TABLE 3: Calculated Vibrational Frequencies (cm^{-1}), IR Intensity (KM/mol), Rotational Constants (MHz), Dipole Moments (Debye), Atomic Charges, and Relative Energies (kcal/mol) of the Species in HFGeS Decomposition Reactions at the B3LYP/6-311G* Level of Theory

species	frequency[a] (IR intensity)	rotational constants	dipole moment	*q*(Ge)	*q*(S)	*q*(F)	*q*(H)	relative energies
$HFGe{=}S$	2150(58), 747(27), 678(129), 553(17), 433(4), 196(16)	A 20673.23 B 3472.37 C 2973.01	2.590	0.6945	−0.2894	−0.4338	0.02873	0.0 (0.0)[b]
HFGeS-A-TS	1772, 562, 487, 387, 142, 1268i							42.51 (43.60)
HFGeS−B-TS-1	1688, 629, 466, 351, 181, 1107i							40.42 (40.47)
trans-FGeSH	2611(7), 691(15), 639(100), 366(60), 363(10), 182(3)	A 11274.66 B 3661.17 C 2763.72	3.055	0.6018	−0.2743	−0.4561	0.1287	−16.80 (−15.99)
HFGeS−B-TS-2	2585, 637, 543, 337, 189, 380i							−7.93 (−7.02)
cis-FGeSH	2621(4), 651(23), 61(68), 367(72), 359(33), 202(8)	A 11071.65 B 3665.34 C 2753.71	1.283	0.6102	−0.3165	−0.4614	0.1676	−17.19 (−16.03)
HFGeS−B-TS-3	1435, 860, 510, 492, 339, 1124i							8.00 (18.63)
HFGeS−C-TS-1	1822, 570, 531, 441, 306, 407i							71.14 (55.16)
trans-HGeSF	1830(212), 687(89), 647(56), 483(8), 380(4), 167(5)	A18807.54 B 2686.39 C 2350.63	2.216	0.1767	0.2384	−0.3599	−0.05526	39.91 (42.37)
HFGeS−C-TS-2	1815, 674, 632, 352, 224, 306i							59.18 (63.05)
cis-HGeSF	1942(175), 687(67), 645(44), 422(0), 370(11), 195(7)	A 11274.66 B 3661.17 C 2763.72	3.055	0.1373	0.2239	−0.3455	−0.01573	42.63 (45.28)
HFGeS−C-TS-3	1067, 611, 512, 459, 210, 1584i							71.82 (74.07)
GeS + HF	GeS: 566(47) HF: 3987(46)	GeS: 5469.38 HF: 617792.85	GeS: 2.513 HF: 2.080					7.90 (−6.40)
FGeS	640(99), 357(1), 106(3)	A 17062.93 B 3512.41 C 2912.80		0.6379	−0.2081	−0.4297		

[a] Without scaling. [b] Values in parentheses are based on the CCSD(T) level of theory; see the text.

pairs and the Ge═S π electrons. Anyhow, all of these results clearly indicate that the HGeSF isomers are unlikely to be observed experimentally.

As one can see in Figure 2, the barriers for the 1,1-HF elimination (A) and 1,2-H migration are comparable. Namely, the CCSD(T) calculations predict that the barrier heights for

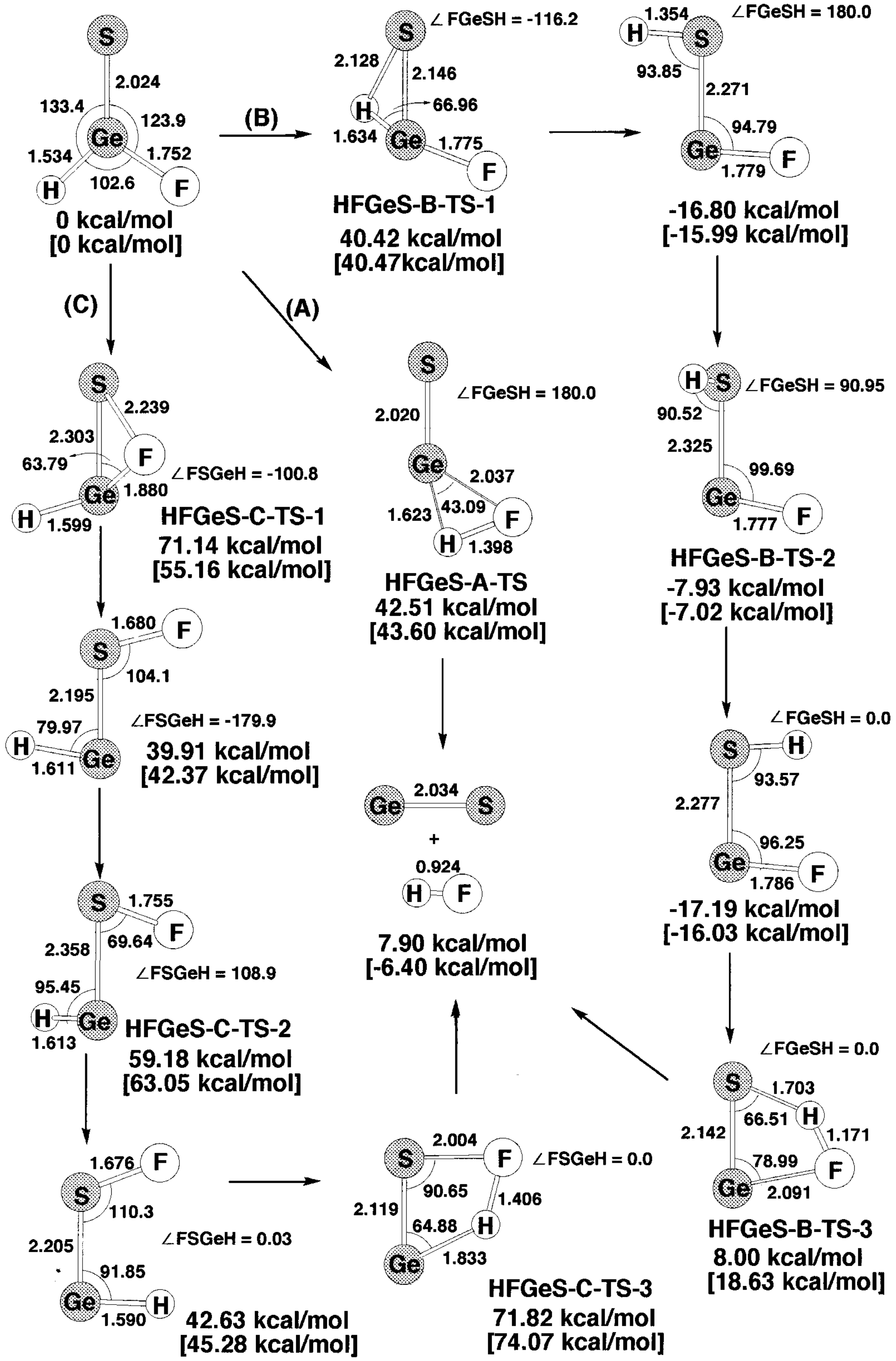

Figure 2. B3LYP/6-311G* optimized geometries (in Å and deg) and relative energies for the HFGe=S isomers. Values in brackets are at the CCSD(T) level of theory (see the text).

reactions (A) and (B) are 43 and 40 kcal/mol, respectively. Thus, the two decomposition reactions are likely to be competitive at high temperatures. In addition, more sizable barriers are present for the radical dissociations of HFGe=S which lead to H + FGeS (D) and F+ HGeS (E); the energies required for these two reactions are at least >68 kcal/mol. In consequence, these calculations suggest that HFGe=S is kinetically stable with respect to the unimolecular decomposition reactions.

Furthermore, as Figure 2 shows, the energies of the HGeSF species are estimated to be about 60 kcal/mol above the FGeSH isomers at the CCSD(T) level of theory. It appears that the following factors are responsible for the large difference in stability between FGeSH and HGeSF. First, singlet FGeSH is stabilized by the polarity of the F−Ge bond, increasing its ionic character and making the germanium more positive. Second, the singlet germylene is stabilized when conjugation of a

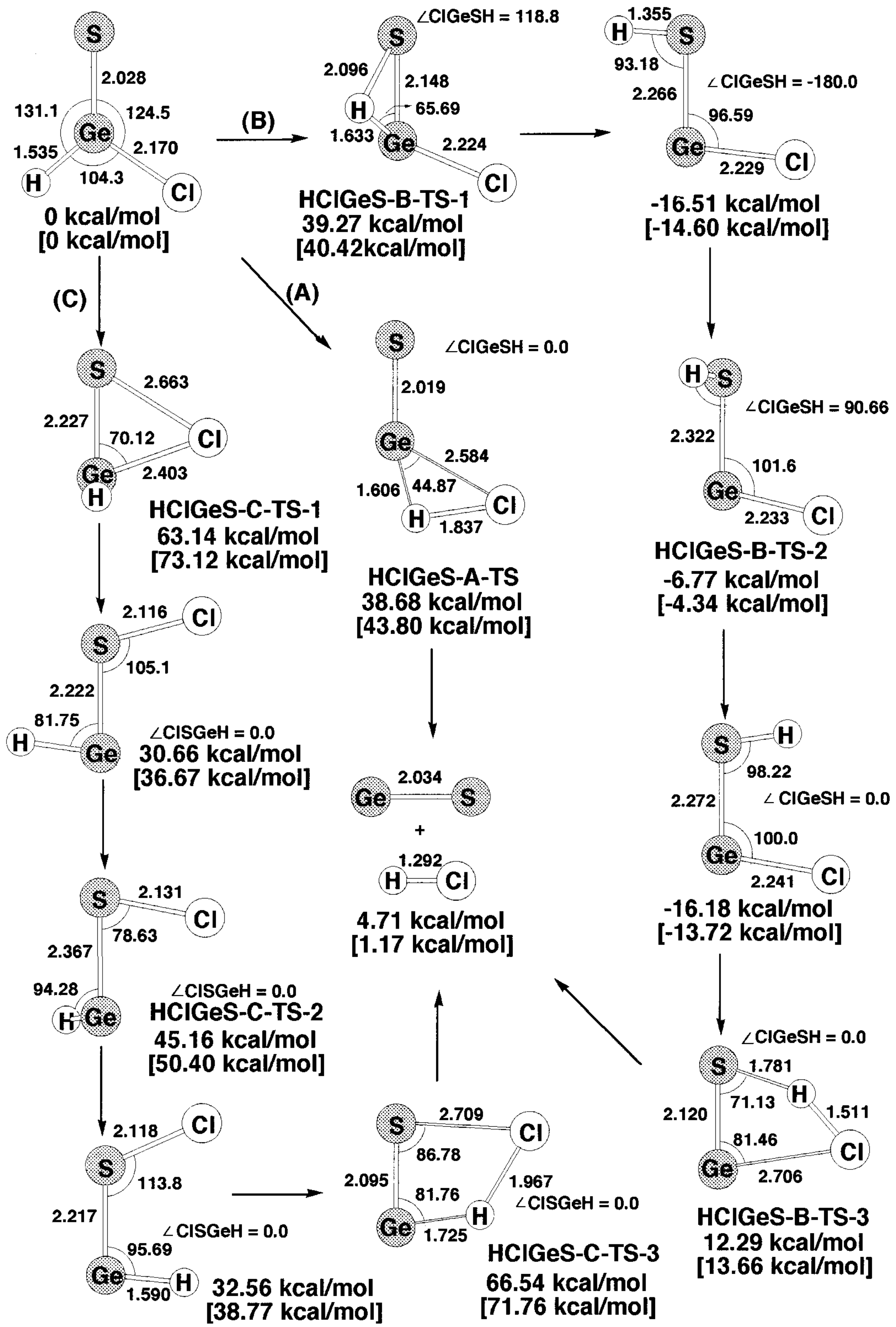

Figure 3. B3LYP/6-311G* optimized geometries (in Å and deg) and relative energies for the HClGe=S isomers. Values in brackets are at the CCSD(T) level of theory (see the text).

heteroatom lone pair is possible. This effect is especially important with a halogen lone pair which possesses a strong π donor character as shown in **1**. In fact, these two explanations of electron-withdrawal and π-donation are readily compatible. Electronegative substituents withdraw electron density from the germanium, making it more positively charged. This increased positive charge makes the germanium a better π-acceptor and, as discussed in a recent report,[6] π-donation from substituents is enhanced. This $n_\pi \rightarrow p_\pi$ delocalization, which can be depicted for FGeSH as shown in **1**, is also responsible for the planar geometries of ClGeSH and BrGeSH (vide infra).

(3) HClGe=S Decomposition Reactions. The B3LYP geometries of the intermediates and transition states of reactions (A−E) are given in Figure 3. The calculated vibrational frequencies as well as dipole moments, rotational constants, atomic charges and relative energies of HClGe=S and its derivatives at both the B3LYP and CCSD(T) levels of theory are collected in Table 4. Unfortunately, no experimental data

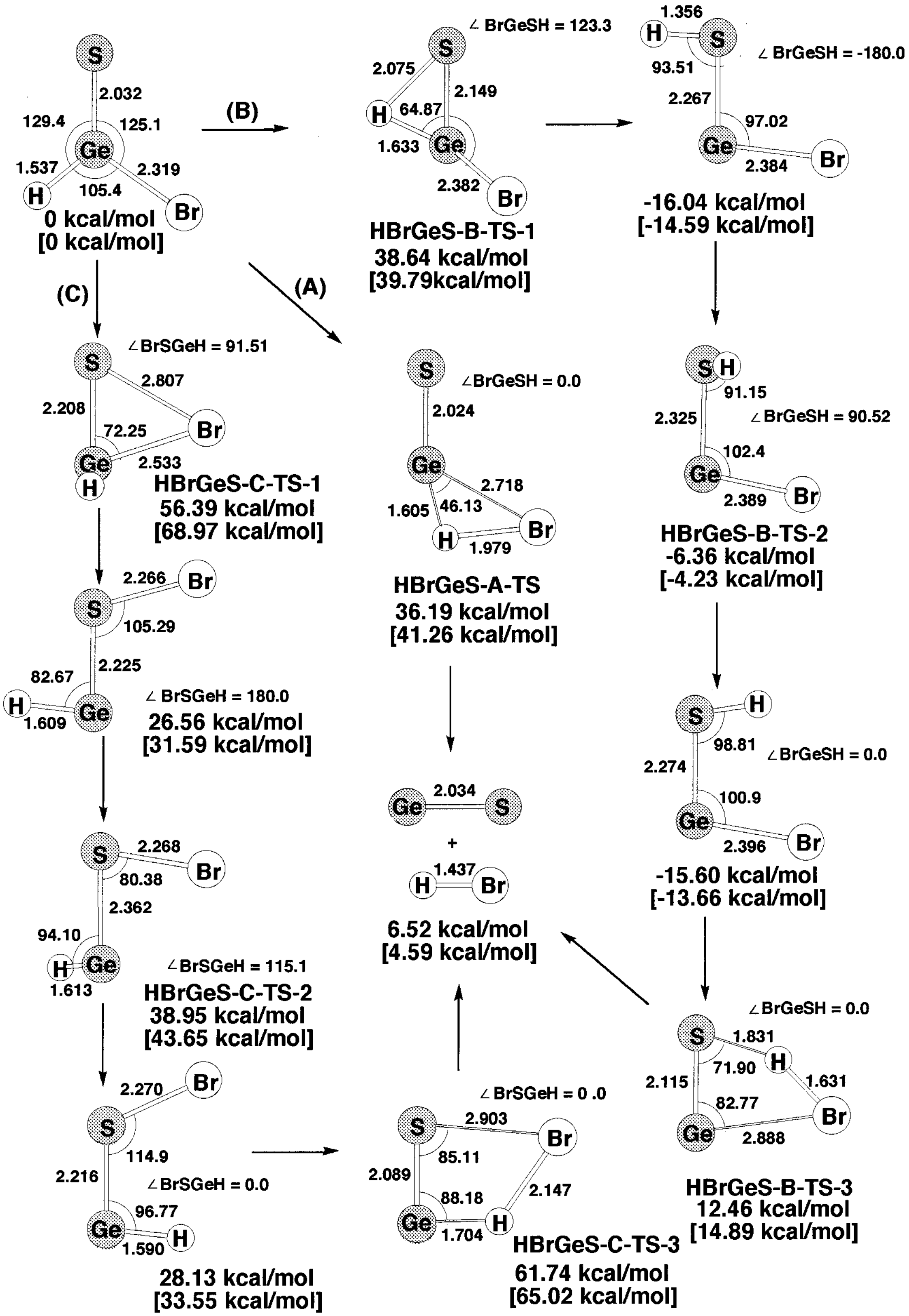

Figure 4. B3LYP/6-311G* optimized geometries (in Å and deg) and relative energies for the HBrGe═S isomers. Values in brackets are at the CCSD(T) level of theory (see the text).

are available in the literature for the HClGeS species. Again, the computational results for the HClGe═S unimolecular reactions are basically similar to those found earlier for the HFGe═S systems. However, three significant results are noteworthy.

First, the CCSD(T) calculations indicate that reaction (A) (i.e., 1,1-HCl elimination) is predicted to be nearly thermoneutral, with an endothermicity of only 1.2 kcal/mol, and to proceed with a sizable barrier of 44 kcal/mol. For reaction pathway (C) (the 1,2-Cl shift), our theoretical calculations predict that the activation energy is 73 kcal/mol which is much larger than for both the 1,1-HCl elimination and the 1,2-H migration reactions (44 and 40 kcal/mol, for reactions (A) and (B), respectively), but lower than for the radical dissociations (67 and 78 kcal/

TABLE 4: Calculated Vibrational Frequencies (cm^{-1}), IR Intensity (KM/mol), Rotational Constants (MHz), Dipole Moments (Debye), Atomic Charges, and Relative Energies (kcal/mol) of the Species in HClGeS Decomposition Reactions at the B3LYP/6-311G* Level of Theory

species	frequency[a] (IR intensity)	rotational constants	dipole moment	q(Ge)	q(S)	q(Cl)	q(H)	relative energies
HClGe═S	2139(58), 717(56), 562(60), 412(1), 390(74), 151(7)	A 13601.82 B 2178.96 C 1878.10	2.420	0.4442	−0.2803	−0.2210	0.05710	0.0 (0.0)(b)
HClGeS-A-TS	1673, 557, 359, 284, 104, 1096i							38.68 (43.80)
HClGeS−B-TS-1	1685, 464, 353, 324, 134, 1141i							39.27 (40.42)
trans-ClGeSH	2604(5), 712(10), 375(41), 363(14), 359(98), 144(2)	A 6436.93 B 2584.96 C 1844.32	3.223	0.3863	−0.2340	−0.2920	0.1396	−16.51 (−14.60)
HClGeS−B-TS-2	2586, 554, 364, 331, 147, 403i							−6.77 (−4.34)
cis-ClGeSH	2622(0), 640(5), 369(47), 353(100), 341(29), 158(5)	A 6520.73 B 2512.58 C 1813.71	1.307	0.4153	−0.2806	−0.3094	0.1748	−16.18 (−13.72)
HClGeS−B-TS-3	1071, 692, 510, 356, 186, 901i							12.29 (13.66)
HClGeS−C-TS-1	1868, 589, 528, 364, 352, 383i							63.14 (73.12)
trans-HGeSCl	1822(211), 669(68) 446(39), 421(2), 368(12), 130(2)	A 11863.21 B 1690.42 C 1479.59	2.353	0.2353	−0.001263	−0.1856	−0.0485	30.66 (36.67)
HClGeS−C-TS-2	1825, 681, 460, 341, 184, 301I							45.16 (50.40)
cis-HGeSCl	1915(168), 657(10), 440(35), 355(1), 348(16), 140(4)	A 14138.51 B 1541.03 C 1389.57	2.463	0.2179	−0.02478	−0.1734	−0.01968	32.56 (38.77)
HClGeS−C-TS-3	1121, 519, 469, 222, 133, 1393i							66.54 (71.76)
GeS + HCl	GeS: 566(47) HCl: 2874(13)	GeS: 5469.38 HCl: 308900.13	GeS: 2.513 HCl: 1.516					4.71 (1.17)
ClGeS	409(23), 343(56), 92(4)	A 11053.66 B 2240.45 C 1862.87	1.588	0.4300	−0.1956	−0.2344		

[a] Without scaling. [b] Values in parentheses are based on the CCSD(T) level of theory; see the text.

mol for reactions (D) and (E), respectively). This indicates that both the 1,2-Cl shifted (C) and the radical dissociations ((D) and (E)) are energetically unfavorable. We thus conclude that neither the HGeSCl species nor the radicals can exist at room temperatures. Moreover, as noted above, our theoretical results suggest that the activation barriers for the reactions (A) and (B) are quite similar, and thus the two reaction routes are likely to be competitive.

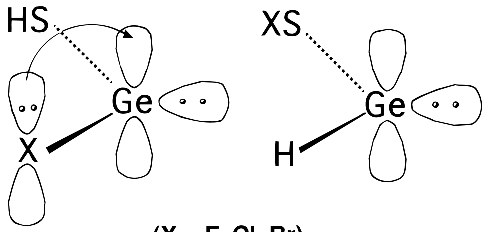

(X = F, Cl, Br)

1

Second, our computational results predict that ClGeSH (the 1,2-H shifted isomer) is about 14 kcal/mol lower in energy than HClGe═S. Moreover, as mentioned above, since the barriers for isomerization from HClGe═S to *trans*-ClGeSH and from *cis*-ClGeSH to HCl + GeS are significantly higher than the rotational barrier from *trans*-ClGeSH to *cis*-ClGeSH, the ClGeSH species should be stable from both kinetic and thermodynamic viewpoints. Thus, once the isomerization barrier is surmounted, HClGe═S will undergo rearrangement leading to the thermodynamically stable product, i.e., the 1,2-H shifted isomer (ClGeSH). However, according to our CCSD(T) calculations, ClGeSH is estimated to be 0.88 kcal/mol more stable in the trans conformer than in the cis form. Such a small energy separation makes the assignment of the ClGeSH singlet state structure uncertain.

Third, as noted above, the activation barriers for the unimolecular decomposition reactions of HClGe═S (such as HCl elimination, isomerization, radical dissociations) are quite large, i.e., at least >40 kcal/mol at the CCSD(T) level of theory. Again, this finding suggests that HClGe═S should be kinetically stable despite its thermodynamic instability.

(4) HBrGe═S Decomposition Reactions. The optimized geometries calculated at the B3LYP/6-311G* level of theory of intermediates and transition states for the reaction channels described in Scheme 1 are summarized in Figure 4. Also, the vibrational frequencies as well as dipole moments, rotational constants and relative energies of HBrGe═S and its derivatives are collected in Table 5. There is as yet no experimental evidence for the existence of HBrGe═S and its derivatives. Again, the calculated potential energy surfaces of the unimolecular reactions of HBrGe═S share many features with those of HFGe═S and HClGe═S as discussed above. However, three intriguing points are worth noting.

First, the single-step elimination of HBr from HBrGe═S (path (A) in Scheme 1) is almost thermoneutral, with a slight endothermicity of 4.6 kca/mol. On the other hand, in the

TABLE 5: Calculated Vibrational Frequencies (cm^{-1}), IR Intensity (KM/mol), Rotational Constants (MHz), Dipole Moments (Debye), Atomic Charges, and Relative Energies (kcal/mol) of the Species in HBrGeS Decomposition Reactions at the B3LYP/6-311G* Level of Theory

species	frequency[a] (IR intensity)	rotational constants	dipole moment	*q*(Ge)	*q*(S)	*q*(Br)	*q*(H)	relative energies
HBrGe═S	2118(65), 712(74), 557(58), 387(1), 288(43), 131(5)	A 11777.61 B 1301.58 C 1172.05	2.427	0.3816	−0.2796	−0.1573	0.05538	0.0 (0.0)[b]
HBrGeS-A-TS	1654, 549, 325, 226, 91, 1020i							36.19 (41.26)
HBrGeS−B-TS-1	1689, 464, 295, 254, 111, 1163i							38.64 (39.79)
trans-BrGeSH	2595(5), 713(6), 368(50), 360(16), 267(51), 120(1)	A 5559.62 B 1531.38 C 1200.66	2.951	0.3449	−0.2396	−0.2451	0.1399	−16.04 (−14.59)
HBrGeS−B-TS-2	2587, 556, 333, 263, 122, 400i							−6.36 (−4.22)
cis-BrGeSH	2627(0), 634(7), 363(60), 339(27), 260(49), 132(3)	A 5666.04 B 1483.00 C 1175.36	1.046	0.3732	−0.2816	−0.2640	0.1724	−15.60 (−13.66)
HBrGeS−B-TS-3	971, 629, 519, 292, 150, 760i							12.46 (14.89)
HBrGeS−C-TS-1	1878, 551, 540, 356, 260, 330i							56.39 (68.97)
trans-HGeSBr	1848(219), 663(82), 411(2), 387(8), 349(18), 103(1)	A 10038.04 B 1023.12 C 928.49	1.925	0.2267	−0.05134	−0.1252	−0.05023	26.56 (31.59)
HBrGeS−C-TS-2	1808, 686, 386, 338, 174, 249i							38.95 (43.65)
cis-HGeSBr	1905(167), 665(7), 386(4), 333(1), 325(19), 112(2)	A 12274.83 B 922.66 C 858.15	2.074	0.2204	−0.07827	−0.1146	−0.02750	28.13 (33.55)
HBrGeS−C-TS-3	1179, 504, 470, 177, 133, 1230i							61.74 (65.02)
GeS + HBr	GeS: 566(47) HBr: 2535(2)	GeS: 5469.38 HBr: 245931.65	GeS: 2.513 HBr: 1.108					6.52 (4.59)
BrGeS	429(9), 248(36), 362(2)	A 10085.18 B 1311.55 C 1160.61	1.507	0.3803	−0.2089	−0.1713		

[a] Without scaling. [b] Values in parentheses are based on the CCSD(T) level of theory; see the text.

multistep isomerizations, BrGeSH (the 1,2-H shifted isomer) is more stable by ~14 kcal/mol than HBrGe═S, but HGeSBr (the 1,2-Br shifted isomer) is less stable than HBrGe═S by ~32 kcal/mol. The barrier separating HBrGe═S and BrGeSH is 40 kcal/mol, while the barrier separating HBrGe═S and HGeSBr is in excess of 43 kcal/mol at the CCSD(T) level. As a consequence, HBrGe═S is kinetically stable toward dissociation to HBr + GeS, either via a one-step (path (A)) or via a stepwise mechanisms (paths (B) and (C)). It should be noted that the activation energies of reactions (A) and (B) are nearly the same (40 kcal/mol at CCSD(T)). Thus, the two reaction pathways are likely to be competitive at high temperatures.

Second, our B3LYP results suggest that the Ge═S bond length of the HXGe═S species correlates with the electronegativity of X and increases as the electronegativity of the substituent decreases. For instance, the Ge═S bond length increases along the series F (2.024 Å) < Cl (2.028 Å) < Br (2.032 Å) < H (2.041 Å). This effect on the length of the Ge═S bond in the germanethiones can be explained in terms of the bond polarity. The Ge═S double bond is polarized, so that the Ge atom is positively charged and the S atom carries a negative charge, i.e., $Ge^{\delta+}{=}S^{\delta-}$. The electron-withdrawing substituents, in particular F, increase the positive charge at germanium[20] (indicated in Tables 2−5 by calculated total net charges) and thus the ionic character of the Ge═S bond. Therefore, the more electronegative the substituent X linked to germanium, the shorter the Ge═S double bond becomes.

SCHEME 2

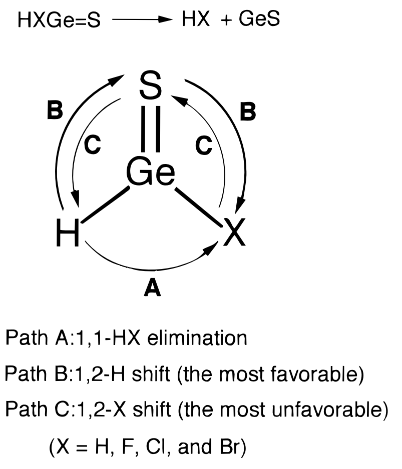

Third, the effect of halogen substitution on the relative stabilities of HXGe═S is interesting. It is clear that the relative stability of the divalent with respect to the doubly bonded species (along the path B) is greatly enhanced when one hydrogen is replaced by a halogen. Moreover, it is apparent that the more electronegative the substituted halogen, the more stable the germylene XGeSH species relative to its corresponding germanethione.

IV. Conclusion

The main conclusions to be drawn from this work are the following:

(1) The overall theoretical results are summarized in Scheme 2. As one can see, our theoretical investigations indicate that the 1,2-hydrogen shift pathway is found to have the lowest

kinetic barriers, while the 1,2-halogen shift route is predicted to have the highest kinetic barrier.

(2) The present calculations predict that the XGeSH molecules (the 1,2-H shifted isomer) have similar stabilities in both trans and cis conformations and that they are much more stable than the HGeSX species (the 1,2-X shifted isomer). This thermodynamic stability is attributed to $n_\pi \rightarrow p_\pi$ delocalization between halogen and germanium, which can greatly stabilize the divalent XGeSH species. We therefore conclude that the monohalogen substituted HGeSX isomers are unlikely to be detected experimentally.

(3) Halogen substitution has a dramatic effect on the competitiveness of the 1,1-HX elimination path and the 1,2-H shift path. In $H_2Ge{=}S$, the 1,1-H_2 elimination has a large energy requirement and will not compete with the 1,2-H shift path. However, it appears that the heavier the substituted halogen in $HXGe{=}S$, the more competitive the 1,1-HX elimination and the 1,2-H migration become.

(4) As in the case of germanone ($HXGe{=}O$),[6] $HXGe{=}S$ is found to be more stable than HGeSX (the 1,2-X shifted isomer) but less stable than XGeSH (the 1,2-H shifted isomer). The relative stability between HGeSX and XGeSH may be due to much stronger XGe bond than HGe bond and comparable strength between SH and SX bonds. Moreover, our theoretical investigation indicates that both XGeSH and HGeSX exist in two conformers separated by a small barrier indicating a fast interconversion process between the cisoid and transoid forms. The former trio have a similar barrier around 10 kcal/mol.

(5) As expected, the calculated potential energy surfaces of the analogous unimolecular reactions of monohalogen substituted $HXGe{=}S$ and $HXGe{=}O$[6] are very similar. In particular, the theoretical results from both systems reveal the fact that germanium is more stable when it bears a lone electron pair than when it is doubly bonded. Nevertheless, our theoretical investigations clearly indicate that $HXGe{=}S$ should be kinetically stable despite its thermodynamic instability.

Acknowledgment. We are very grateful to the National Center for High-Performance Computing of Taiwan and the Computing Center at Tsing Hua University for generous amounts of computing time. We also thank the National Science Council of Taiwan for their financial support. We thank the reviewers for their helpful suggestions in improving the manuscript.

References and Notes

(1) For reviews, see: (a) Barrau, J.; Escudie, J.; Stagé, J. *Chem. Rev.* **1990**, *90*, 283. (b) Barrau, J.; Rima, G. *Coord. Chem. Rev.* **1998**, *178*, 593. (c) Esoudié, J.; Couret, C.; Ranaivonjatovo, H.; Stagé, J. *Coord. Chem. Rev.* **1994**, *130*, 427. (d) Esoudié, J.; Couret, C.; Ranaivonjatovo, H. *Coord. Chem. Rev.* **1998**, *178*, 565. (e) Tokitoh, N.; Matsumoto, T.; Okazaki, R. *Bull. Chem. Soc. Jpn.* **1999**, *72*, 1665.

(2) (a) Leigh, W. J. *Pure Appl. Chem.* **1999**, *71*, 453. (b) Tokitoh, N. *Pure Appl. Chem.* **1999**, *71*, 495.

(3) Windus, T. L.; Gordon, M. S. *J. Am. Chem. Soc.* **1992**, *114*, 9559.

(4) Galbraith, J. M.; Schaefer III, H. F. *J. Mol. Struct.* (*Theochem*) **1998**, *424*, 7.

(5) Boone, A. J.; Magers, D. H.; Leszczyñski, J. *Int. J. Quantum Chem.* **1998**, *70*, 925.

(6) Lin, C.-L.; Su, M.-D.; Chu, S.-Y. *Chem. Phys.* **1999**, *249*, 145.

(7) (a) Veith M.; Becker, S.; Huch, V. *Angew. Chem., Int. Ed. Engl.* **1989**, *28*, 1237. (b) Barrau, J.; Rima, G.; Amraoui, T. E. *J. Organomet. Chem.* **1998**, *570*, 163.

(8) (a) Veith, M.; Detemple, A.; Huch, V. *Chem. Ber.* **1991**, *124*, 1135. (b) Suzuki, H.; Tokitoh, N.; Okazaki, R.; Nagase, S.; Goto, M. *J. Am. Chem. Soc.* **1998**, *120*, 11096.

(9) (a) Barrau, J.; Balaji, V.; Michi, J. *Organometallics* **1989**, *8*, 2034. (b) Köppe, R.; Schnöckel H. *Z. Anorg. Allg. Chem.* **1991**, *592*, 179. (c) Ossig, G.; Meller, A.; Bronneke, C.; Muller, O.; Schaefer, M.; Herbst-Irmer, R. *Organometallics* **1997**, *16*, 2116.

(10) (a) Bodiquel, J.; Meunier, P.; Kubicki, M. M.; Richard, P.; Gautheron, B. *Organometallics* **1992**, *11*, 1423. (b) Lavayssiere, H.; Stage, J.; Barrau, J.; Traore, M. *J. Organomet. Chem.* **1982**, *240*, 335.

(11) (a) Tokitoh, N.; Kishikawa, K.; Manmaru, K.; Okazaki, R. *Heterocycles* **1997**, *44*, 149. (b) Tokitoh, N.; Matsumoto, T.; Okazaki, R. *Heterocycles* **1995**, *40*, 127. (c) Tokitoh, N.; Mastsumoto, T.; Manmaru, K.; Okazaki, R. *Tetrahedron Lett.* **1991**, *32*, 6877.

(12) (a) Tokitoh, N.; Mastsumoto, T.; Manmaru, K.; Okazaki, R. *J. Am. Chem. Soc.* **1993**, *115*, 8855. (b) Matsumoto, T.; Tokitoh, N.; Okazaki, R. *J. Am. Chem. Soc.* **1999**, *121*, 8811.

(13) Trinquier, G.; Pleissier, M. *J. Organomet. Chem.* **1981**, *214*, 169.

(14) Trinquier, G.; Barthelat, J.; Stagé, J. *J. Am. Chem. Soc.* **1982**, *104*, 5931.

(15) So, S. P. *J. Phys. Chem.* **1993**, *97*, 4643.

(16) Nowek, A.; Sims, R.; Babinec, P.; Leszczyñski, J. *J. Phys. Chem. A* **1998**, *102*, 2189.

(17) Frisch, M. J.; Trucks, G. W.; Schlegel, H. B.; Scuseria, G. E.; Robb, M. A.; Cheeseman, J. R.; Zakrzewski, V. G.; Montgomery, J. A., Jr.; Stratmann, R. E.; Burant, J. C.; Dapprich, S.; Millam, J. M.; Daniels, A. D.; Kudin, K. N.; Strain, M. C.; Farkas, O.; Tomasi, J.; Barone, V.; Cossi, M.; Cammi, R.; Mennucci, B.; Pomelli, C.; Adamo, C.; Clifford, S.; Ochterski, J.; Petersson, G. A.; Ayala, P. Y.; Cui, Q.; Morokuma, K.; Malick, D. K.; Rabuck, A. D.; Raghavachari, K.; Foresman, J. B.; Cioslowski, J.; Ortiz, J. V.; Stefanov, B. B.; Liu, G.; Liashenko, A.; Piskorz, P.; Komaromi, I.; Gomperts, R.; Martin, R. L.; Fox, D. J.; Keith, T.; Al-Laham, M. A.; Peng, C. Y.; Nanayakkara, A.; Gonzalez, C.; Challacombe, M.; Gill, P. M. W.; Johnson, B. G.; Chen, W.; Wong, M. W.; Andres, J. L.; Head-Gordon, M.; Replogle, E. S.; Pople, J. A. *Gaussian 98*; Gaussian, Inc.: Pittsburgh, PA, 1998.

(18) (a) Lee, C.; Yang, W.; Parr, R. G. *Phys. Rev.* **1988**, *B37*, 785. (b) Becke, A. D. *J. Chem. Phys.* **1993**, *98*, 5648. (c) Stephens, P. J.; Devlin, F. J.; Chabalowski, C. F.; Frisch, M. J. *J. Phys. Chem.* **1994**, *98*, 11623.

(19) (a) Lee, T. J.; Scuseria, G. *Quantum Mechanical Electronic Structure Calculations with Chemical Accuracy*; Langnoff, S. F., Ed.; Kluwer Academic Press: Dordrecht, The Netherlands, 1995. (b) Raghavachari, K.; Trucks, G. W.; Pople, J. A.; Head-Gordon, M. *Chem. Phys. Lett.* **1989**, *157*, 479.

(20) (a) Wiberg, K. B. *Acc. Chem. Res.* **1999**, *32*, 922. (b) Wiberg, K. B. *J. Chem. Educ.* **1996**, *73*, 1089.